Proceedings of the 3rd Croatian Conference on Earthquake Engineering - 3CroCEE
19–22 March 2025, Split, Croatia

DOI: https://doi.org/10.5592/CO/3CroCEE.2025.105

BEHAVIOUR OF DUAL STEEL FRAMES WITH INNOVATIVE DOUBLE SKIN COLD-FORMED STEEL CONCRETE COMPOSITE SHEAR WALLS

Ivan Lukačević[(1)], Emanuel Krupa-Jurić [(2)], Ivan Ćurković [(3)], Marko Barišić [(4)]

[(1)] *Associate Professor, University of Zagreb, Faculty of Civil Engineering, ivan.lukacevic@grad.unizg.hr*
[(2)] *Research Assistant, University of Zagreb, Faculty of Civil Engineering, emanuel.krupa.juric@grad.unizg.hr*
[(3)] *Assistant Professor, University of Zagreb, Faculty of Civil Engineering, ivan.curkovic@grad.unizg.hr*
[(4)] *PhD Student, University of Zagreb, Faculty of Civil Engineering, marko.barisic@student.grad.unizg.hr*

Abstract

Dual systems that combine moment-resisting frames with innovative replaceable bracing systems offer significant advantages over conventional solutions. The key benefits of these systems include energy dissipation at specific locations and a re-centring capability, which substantially reduces repair costs. However, the design of such systems must meet specific requirements, such as using higher steel grades to ensure the part of the system remains elastic and structural solutions for the double skin cold formed shear wall filled with concrete, which ensures the system's ductile behaviour. This paper presents an assessment of a dual system using finite element analysis that integrates a moment-resisting multi-story frame with an innovative double-skin cold-formed steel concrete composite shear wall. The steel frame consists of three bays, with a central bay being a braced frame and two adjacent bays being moment-resisting frames. The shear wall, acting as a bracing system, consists of corrugated cold-formed steel sheets filled with concrete, which are connected with intermediate shear connectors and form a sandwich steel-concrete-steel panel. In the first step, non-linear analyses of individual shear wall panels are conducted considering influences of steel sheet thickness, concrete strength and type of shear connection. Afterwards, pushover analyses are performed using the resulting load-displacement behaviour of the analysed shear walls. The performance of the analysed systems is discussed in terms of collapse mechanisms, capacity curves, overstrength ratios, behaviour factors, and potential improvements for the shear wall's performance. The analysed systems demonstrated their dual behaviour and re-centring capabilities, but further research on different shear wall typologies will provide deeper insights into their practical applications.

Keywords: dual systems, re-centring capability, cold-formed steel double skin concrete shear walls, non-linear static pushover method, capacity curve, overstrength ratio, collapse mechanism

1. Introduction

Modern codes require ductile behaviour during earthquakes and seismic energy dissipation through inelastic deformation. The capacitive design ensures seismic energy dissipation through the yielding of structural components at specific locations within the structure. Even though inelastic deformations are localised, damage is irreversible, and repair is complex, sometimes even impossible. In addition, the repair costs could be very high. A possible solution can be found to improve the stated issues when applying dual systems. The idea of dual systems, formed by combining moment-resisting frames (MRF) and replaceable bracing systems, is that seismic energy is dissipated through the yielding of the bracing system while MRFs remain elastic and enable re-centering of the structure. MRF design may require higher-grade steel to ensure elastic behaviour, while the bracing system must be sufficiently rigid and ductile [1]. In [2] the authors summarised the experimental and numerical behaviour of re-centring dual eccentrically braced frames (EBFs) with removable links. Experimental tests on full-scale dual eccentrically braced structures were conducted to test the re-centring capability and feasibility of the link removal. Results showed excellent behaviour at serviceability limit state (SLS) and ultimate limit state (ULS) earthquakes. Small permanent deformations were observed but within the erection tolerance. Two case study buildings were evaluated using pushover analysis. The analysis showed that MRFs remained elastic before reaching ULS deformations in the removable links of the EBF, which confirmed the dual behaviour of the structures. In paper [3] the authors investigate replaceable shear

DOI: https://doi.org/10.5592/CO/3CroCEE.2025.105

panels as lateral load-resisting and dissipative systems as alternatives to traditional systems. The results showed that shear panels are efficient bracing systems with stable cyclic behaviour and good ductility. The analysis showed that yielding occurs in replaceable shear panels while MRFs remain elastic. Also, re-centering analysis showed that residual drift is not present after unloading. However, slender shear panels may buckle during the early stages of lateral loading.

Also, a possible solution for lateral stabilisation can be the usage of different composite steel-concrete systems. Combining concrete and steel can achieve both rigidity and ductility of the bracing system [4]. Composite systems, where steel sheets are connected with screws, bolts, or diaphragms and filled with concrete first saw used in the nuclear industry and steel frames of highrise buildings. Such systems showed excellent behaviour regarding lateral resistance and ductility. One of the ways of optimal use of materials is the application of cold-formed steel profiles and elements. In papers [5,6], the application of corrugated steel sheets was investigated, and it was shown that corrugated sheets provide greater resistance and stiffness than conventional steel sheets. However, in highly seismic areas for the stabilisation of medium-rise and highrise buildings, the disadvantage of such systems is insufficient shear resistance, which can be increased by introducing concrete. In paper [7], the authors conducted a numerical analysis which showed potentially favourable characteristics of a shear wall composed of corrugated steel sheets and concrete.

This paper presents an assessment of dual systems, based on finite element analysis, that integrates multi-story MRFs with innovative double-skin cold-formed steel concrete composite shear walls. In the first step, non-linear analyses of individual shear wall panels are conducted considering influences of steel sheet thickness, concrete strength, and shear connection type. Afterwards, pushover analyses are performed using the resulting load-displacement behaviour of the analysed shear walls.

2. Analysed system

The structure consists, in the x direction, of two three-bay moment resisting frames with the shear walls in the central bay and in the y direction of four one-bay moment resisting frames, of which two with the bracing system. The shear wall, acting as a bracing system, consists of corrugated cold-formed steel sheets filled with concrete, which are connected with intermediate shear connectors and form a sandwich steel-concrete-steel panel.

The structure has eight floors with a floor height of 4,2 m, and the span of the bay is 8 m. The structure is regular in plan and height, as shown in Figs. 1. and 2. In addition, Fig. 2. shows the schematic view of the structure's re-centering capability.

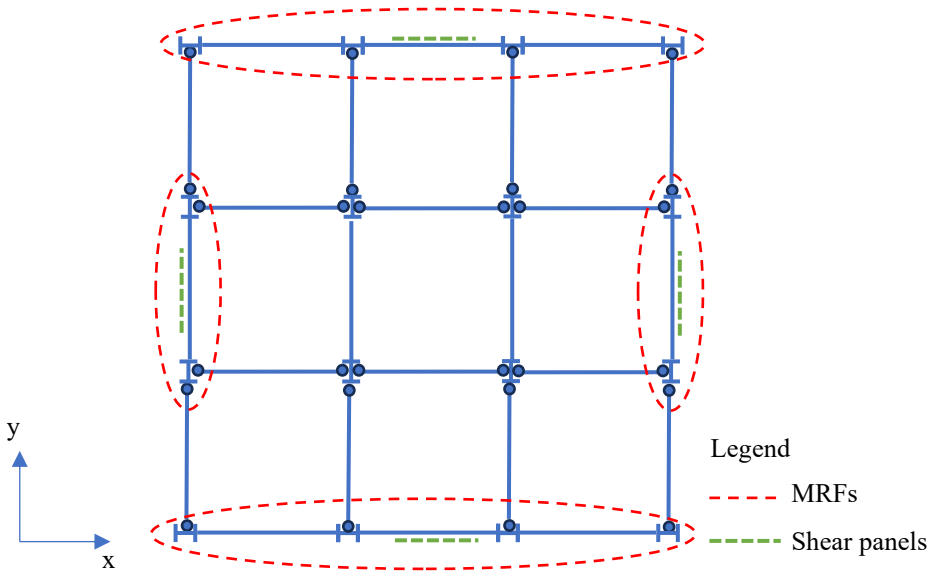

Figure 1. Building plan

DOI: https://doi.org/10.5592/CO/3CroCEE.2025.105

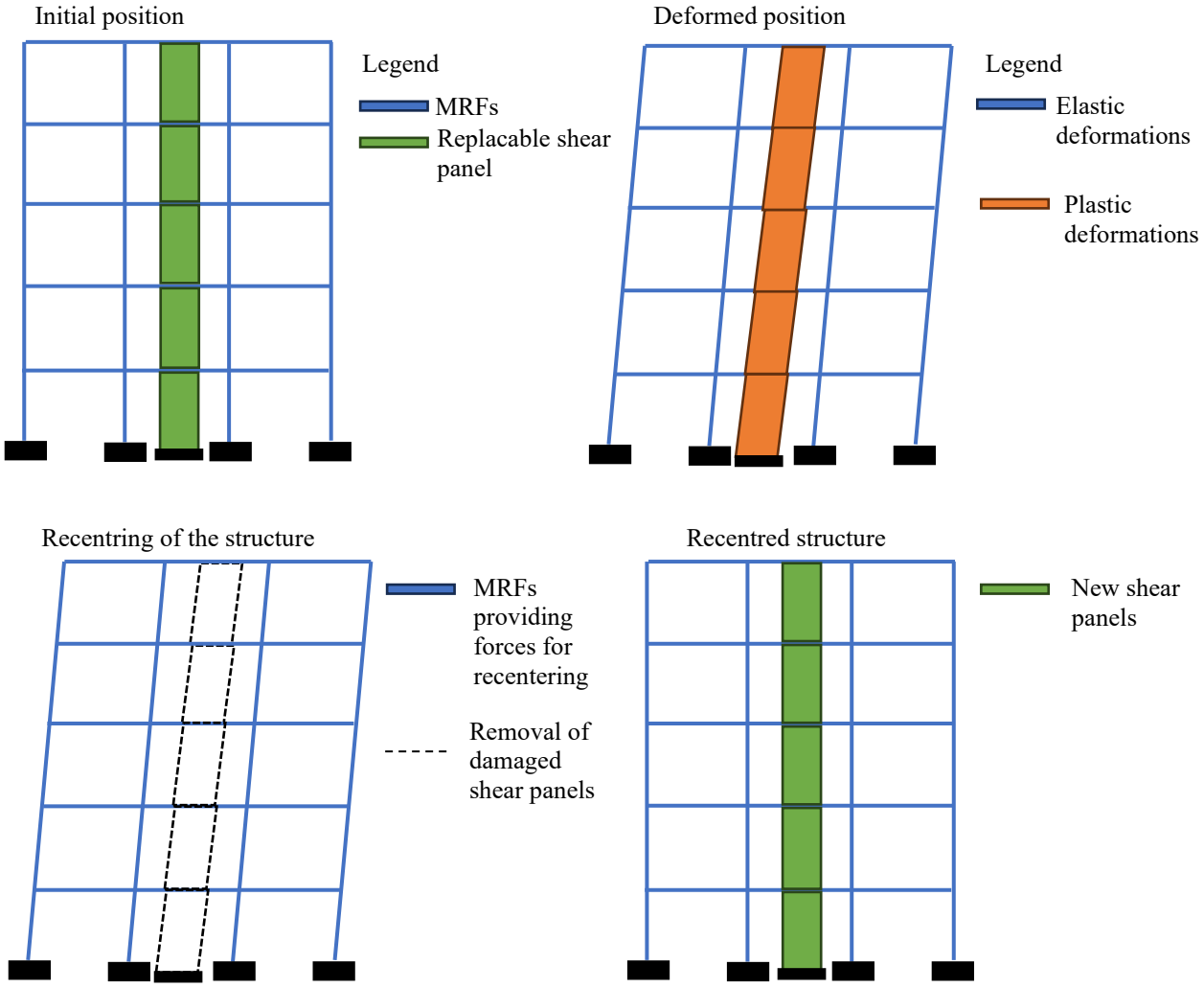

Figure 2. Building elevation and schematic view of the structure's re-centering capability

3. Numerical analysis of the shear wall

Numerical analysis of composite shear walls was performed with Abaqus software [8] by using Explicit Solver.

3.1. Geometry and Components

The shear wall consists of double skin cold formed corrugated steel sheets filled with concrete, which are connected with intermediate shear connectors forming a sandwich steel-concrete-steel panel, as shown in Fig. 4. The shear wall is 2.2 m wide and 4.2 m tall with an average thickness of 120 mm. Details regarding geometry are provided in [9]. Cold-formed corrugated steel sheets were modelled using homogenous shell elements, type S4R and the concrete slab was modelled using homogenous solid elements, type C3D8R. Intermediate shear connectors were modelled using beam elements B31.

3.2. Material

All materials were assigned elastic and plastic behaviour. Material properties of steel used for corrugated sheets were obtained by experimental tests [10]. The elastic behaviour of steel was modelled as isotropic with Young's modulus equal to E = 210 000 MPa and Poisson's ratio of ν = 0.3. Plastic material properties were modelled using a true stress-strain relationship.

DOI: https://doi.org/10.5592/CO/3CroCEE.2025.105

The elastic behaviour of the concrete was modelled as isotropic with Young's modulus equal to $E = 31\,476$ MPa and $E = 32\,836$ MPa for classes of concrete C25/30 and C30/37, respectively and Poisson's ratio of $v = 0.2$. The plastic behaviour of the concrete was simulated with the Concrete Damage Plasticity (CDP) model according to research provided in paper [11].

3.3. Boundary conditions and interactions

At the bottom of the shear wall, displacements and rotations in all three directions are prevented at all points of the corrugated steel sheet. At the top of the shear wall, out-of-plane displacement is prevented. Also, all points of the corrugated steel sheet edge are connected using the coupling constraints with a reference point through which the horizontal load was applied using the displacement control method.

The shear connection between concrete and corrugated steel sheets is realised with bolts embedded in the concrete and a "tie constraint" corresponding to a full shear connection. "MPC constraint"-Multi-point constraints were used to attach bolts to corrugated steel sheets.

Contact between bolts and concrete was modelled with tangential behaviour with a friction coefficient equal to 0.3 and normal behaviour as "hard" contact.

3.4. Mesh convergence analysis

A mesh sensitivity test was conducted to determine the influence of mesh size on the results. Varied mesh sizes are 5, 10, 15, and 25 mm for the corrugated steel sheets and 10, 15, 20, 25, and 50 mm for the concrete filling. The results are presented with a force-displacement curve shown in Fig. 3. Table 1 shows the ultimate force P_u and displacement u_u for models with different mesh sizes

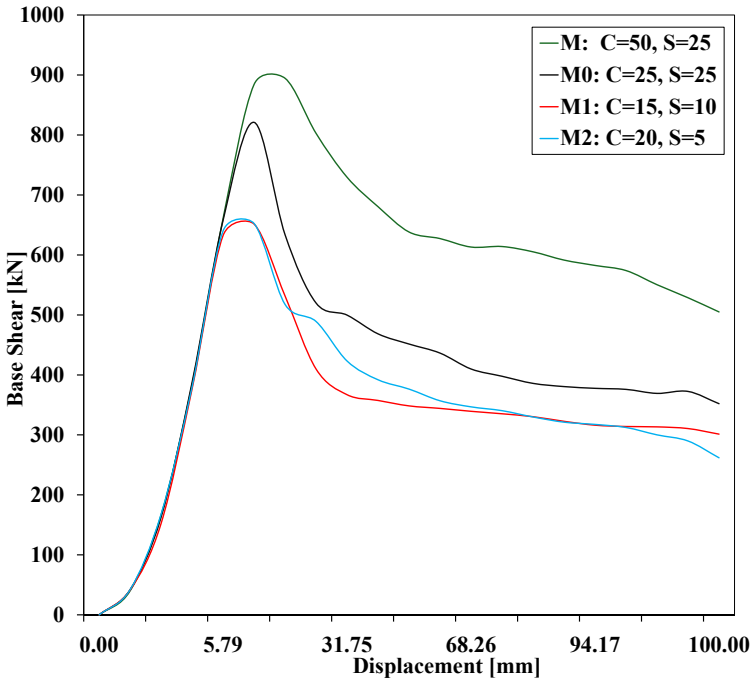

Figure 3. Comparison of the force-displacement curves for different mesh sizes

Table 1. Models with different mesh sizes and corresponding ultimate force and displacement

MODEL	MESH	P_u [kN]	u_u [mm]
CCFSSW_03_03_16_M	CCFS-25, C-50	894,47	16,32
CCFSSW_03_03_16_M0	CCFS-25, C-25	821,00	10,36
CCFSSW_03_03_16_M1	CCFS-10, C-15	651,60	10,34
CCFSSW_03_03_16_M2	CCFS-5, C-20	652,46	10,35

Proceedings of the 3rd Croatian Conference on Earthquake Engineering - 3CroCEE
19–22 March 2025, Split, Croatia

DOI: https://doi.org/10.5592/CO/3CroCEE.2025.105

The optimal mesh size is determined by considering the convergence of the results. Models with a mesh configuration denoted CCFSSW_03_03_16_M and CCFSSW_03_03_16_M0 have significant deviations in the results. Convergence of results is observed for models with a mesh configuration denoted CCFSSW_03_03_16_M1 and CCFSSW_03_03_16_M2. Therefore, the adopted mesh configuration is CCFSSW_03_03_16_M1.

3.5. Parametric analysis

In order to determine the optimal structural design of the shear wall, parametric analysis was performed. The assumption is that the following parameters mostly influence the behaviour of the shear wall: the thickness of the corrugated steel sheets, concrete strength, the diameter of the bolts and the arrangement of the bolts. Therefore, these parameters were varied. Also, the influence of mesh sensitivity on the results was tested. The behaviour of each analysed shear wall is represented with a numerical load-displacement curve. Table 2 lists all varied parameters and Fig. 4. shows different cases of bolt arrangement.

Table 2. Parameters varied within the parametric study

Steel sheet thickness	Concrete strength	Diameter of bolts	Shear connection type
1 mm, 3 mm	C25/30, C30/37	M12, M16	SW1, SW2, SW3

The influence of the parameter change is best seen by comparing numerical force-displacement curves. In a comparison of the results for different shear connection types and bolt arrangements, shown in Fig. 5. a), it can be concluded that the shear wall with bolt configuration SW2 has the greatest capacity, followed by a shear wall with full shear connection. In contrast, the shear wall with bolt arrangement SW3 has the lowest capacity. A larger bolt diameter leads to a slight increase in the shear wall's capacity, as represented in Fig. 5. b).

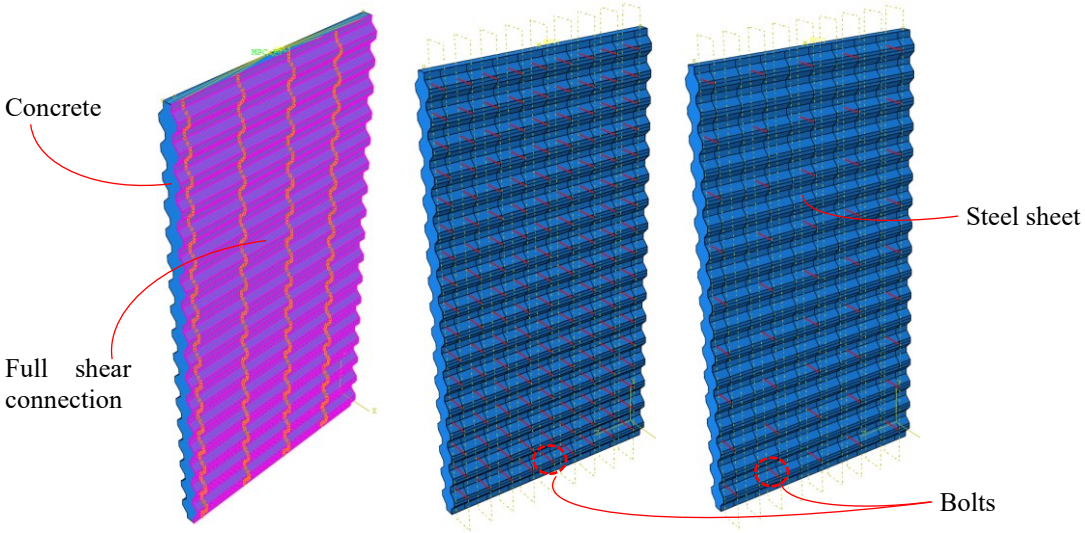

Figure 4. Type of the shear connection and bolt arrangement SW1, SW2 and SW3 in the given order

By comparing numerical force-displacement curves of the shear walls with the same bolt arrangement and diameter, shown in Fig. 5. c), it can be seen that the highest capacity has the shear wall with concrete strength C30/37 and steel sheet thickness of 3 mm, followed by the shear wall with concrete strength C25/30 and steel sheet thickness of 3 mm. The lowest capacity shear wall is composed of concrete strength C25/30 and a steel sheet thickness of 1 mm.

Based on the parametric study, the increase in the strength of the concrete and the type of the shear connection makes the most significant contribution to the capacity of the shear wall. In contrast, the

DOI: https://doi.org/10.5592/CO/3CroCEE.2025.105

increase in the thickness of the steel sheets and bolt diameter results with a minor contribution to the wall strength.

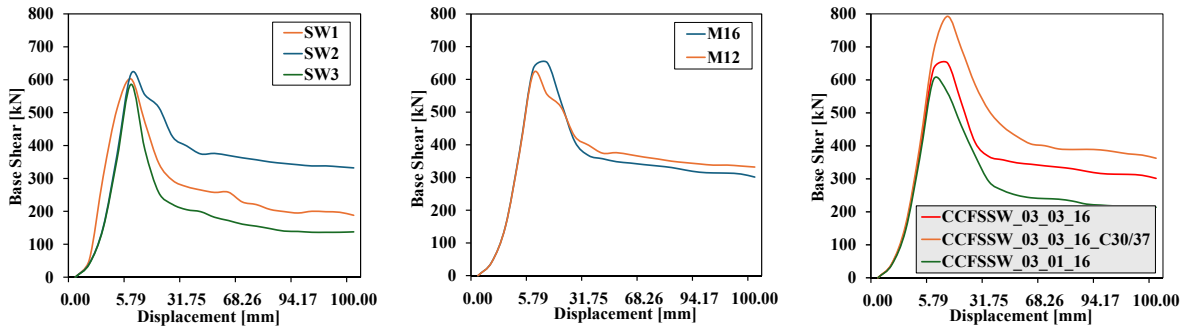

a) b) c)

Figure 5. a) Influence of the shear connection type, b) Influence of the bolt diameter on the capacity of the shear wall, c) Influence of the concrete strength and steel sheet thickness on the capacity of the shear wall

4. Seismic analysis

4.1. Selection of the analysis method

For performance-based design and damage control, the most suitable are non-linear methods. Therefore, the non-linear static (pushover) method will be used. Furthermore, pushover analysis gives better insight into the structure's behaviour than the conventional approach using elastic response spectrum reduced with behaviour factor q for several reasons. First, values of behaviour factors are approximate and may not be suitable for specific structures. Analysis based on the q factor does not consider redistribution of internal forces and deformation when inelastic deformations occur [12]. Moreover, the collapse mechanism cannot be predicted using the elastic distribution of forces and deformations. The assessment of the structure behaviour has been done using the non-linear static (pushover) method - N2 method. The analysis results ar provided as a characteristic force-displacement relationship that gives key information about structure: strength, stiffness and ductility.

4.2. Overview of the N2 method

The steps of the N2 method, according to [13], are:

1. Data

The analysis begins by defining the 2D structural model, the force-deformation relationship for structural elements, and seismic demand, which is determined in the form of an elastic pseudo-acceleration spectrum where spectral acceleration is a function of the period of the structure.

2. Seismic demand in Acceleration-displacement format

The acceleration response spectrum is transformed into AD format using the following relation:

$$S_{de} = \frac{T^2}{4\pi^2} S_{ae} \tag{1}$$

where S_{de} and S_{ae} are values of displacement and acceleration, respectively, corresponding to the response spectrum in AD format for a fundamental period and fixed viscous damping ratio.

For an inelastic Single degree of freedom (SDOF) system with a bilinear force-deformation relationship, the acceleration spectrum and the displacement spectrum can be determined using the following relations:

$$S_a = \frac{f_y}{m} = \frac{S_{ae}}{R_\mu} \tag{2}$$

Proceedings of the 3rd Croatian Conference on Earthquake Engineering - 3CroCEE
19–22 March 2025, Split, Croatia

DOI: https://doi.org/10.5592/CO/3CroCEE.2025.105

$$S_d = \frac{\mu}{R_\mu} S_{de} = \frac{\mu}{R_\mu} \frac{T^2}{4\pi^2} S_{ae} = \mu \frac{T^2}{4\pi^2} S_a \tag{3}$$

where μ is the ductility factor and R_μ is the reduction factor due to ductility.

For determining R_μ, factor concerning the period T, N2 method, as implemented in EC8, uses bilinear relation between R_μ and T:

$$R_\mu = (\mu - 1)\frac{T}{T_c} + 1; T < T_c \tag{4}$$

$$R_\mu = \mu; T \geq T_c \tag{5}$$

where T_c is the transition period of the short-period range and the medium-period range.

In the medium-period and long-period range, the equal displacement rule applies as stated in equation (5). Now, the demand spectra in AD format can be obtained.

3. Pushover analysis

The structure is subjected to a monotonically increasing pattern of lateral forces and constant gravitational load. Lateral forces represent inertial forces due to earthquakes. There is no exact solution for the distribution of lateral forces. A reasonable solution is to use two different displacement shapes and to envelop the results. Commonly used load patterns are uniform and modal distribution. The main assumption of the method is that the structure vibrates in a single time-invariant mode. Therefore, the modal distribution of lateral forces would equal the effective (inertial) forces acting upon the structure during an earthquake. It is important to emphasise that this method is not applicable to structures that vibrate in higher modes. The vector of lateral loads is:

$$P = p\boldsymbol{\Psi} = p\boldsymbol{M}\boldsymbol{\Phi} \tag{6}$$

where p controls magnitude. Distribution of lateral forces $\boldsymbol{\Psi}$ related to diagonal mass matrix $\boldsymbol{M}$ and assumed displacement shape $\boldsymbol{\Phi}$.

Loading of a structure is displacement-controlled, i.e., the load is applied until predefined displacement is achieved. By incrementally increasing the load, elements progressively yield, leading to overall stiffness loss. The analysis results in a characteristic non-linear force-displacement curve, most commonly related to base shear and rooftop displacement.

4. Equivalent SDOF system

In the N2 method, seismic demand is determined by using response spectra given for SDOF systems, and the Multi degree of freedom (MDOF) system has to be transformed into an equivalent SDOF system.

The equation of motion of the MDOF system is:

$$\boldsymbol{M}\ddot{\boldsymbol{U}} + \boldsymbol{R} = \boldsymbol{M}\boldsymbol{1}a \tag{7}$$

where $\boldsymbol{M}$ is a diagonal mass matrix, and $\boldsymbol{U}$ and $\boldsymbol{R}$ are displacement and internal forces vectors, respectively. 1 is the unit vector and a is the ground acceleration. Dumping is included in the design spectrum. When assuming a constant displacement shape, the displacement vector $\boldsymbol{U}$ is defined as:

$$\boldsymbol{U} = \boldsymbol{\Phi} D_t \tag{8}$$

where D_t is time-dependent top displacement. $\boldsymbol{\Phi}$ is normalised such that the top component is equal to 1.

Equilibrium of forces:

Proceedings of the 3rd Croatian Conference on Earthquake Engineering - 3CroCEE
19–22 March 2025, Split, Croatia

DOI: https://doi.org/10.5592/CO/3CroCEE.2025.105

$$\boldsymbol{P} = \boldsymbol{R} \tag{9}$$

where R represents internal forces and P statically applied external forces.

Expanding equation (9) and multiplying from the left-hand side with Φ^T the following equation is obtained:

$$\boldsymbol{\Phi^T M \Phi \ddot{D}_t} + \boldsymbol{\Phi^T M \Phi} p = -\boldsymbol{\Phi^T M 1} a \tag{10}$$

Dividing the left-hand side with $\boldsymbol{\Phi^T M 1}$, equation of motion of equivalent SDOF system is:

$$m^* \ddot{D}^* + F^* = -m^* a \tag{11}$$

Where m^* is the mass of the equivalent SDOF system:

$$\sum_i^n m_i^* \cdot \Phi_i \tag{12}$$

and D^* and F^* are the displacement and force of the equivalent SDOF system:

$$D^* = \frac{d_t}{\Gamma} \tag{13}$$

$$F^* = \frac{V}{\Gamma} \tag{14}$$

Base shear of the MDOF system:

$$V = \{\Phi\}^T [M]\{1\} p = p m^* \tag{15}$$

The constant Γ of transformation of the MDOF system to the SDOF system and vice versa is defined as:

$$\Gamma = \frac{\{\Phi\}^T [M]\{1\}}{\{\Phi\}^T [M]\{\Phi\}} = \frac{\sum m_i \Phi_i}{\sum m_i \Phi_i^2} \tag{16}$$

Constant Γ is applied for the transformation of both displacements and forces, as shown in equations (13) and (14), force-displacement curve of the equivalent SDOF system has the same shape and initial stiffness as one for the MDOF system. The obtained force-displacement curve of equivalent SDOF is then simplified to a bilinear elastoplastic curve. To determine the initial stiffness of the idealised system, EC8 suggests using the principle of equal energy of the real and idealised curve. The period of the idealised system can be determined as follows:

$$T^* = 2\pi \sqrt{\frac{m^* d_y^*}{F_y^*}} \tag{17}$$

where d_y^* and F_y^* are yield displacement and yield force, respectively. Finally, the capacity diagram in AD format is obtained using the following equation:

$$S_a = \frac{F^*}{m^*} \tag{18}$$

5. Seismic demand

Seismic demand can be determined using a graphical procedure by plotting demand spectra, inelastic spectra in AD format, obtained from elastic demand spectra using ductility factor, and capacity diagram

DOI: https://doi.org/10.5592/CO/3CroCEE.2025.105

in the same graph, presented in Figs. 6. a) and 6. b). Elastic demand is determined by the intersection of the radial line corresponding to the elastic period of the idealised bilinear system, T^*, with elastic demand spectra. Inelastic displacement demand depends on the period of the system.

For periods shorter than T_c, inelastic displacement demand can be determined using the following relation:

$$S_d = \mu D_y^* = \frac{S_{de}}{R_\mu}\left(1 + (R_\mu - 1)\frac{T_C}{T^*}\right) \tag{19}$$

For periods larger than T_c, the equal displacement rule applies, i.e.:

$$S_d = S_{de}(T^*) \tag{20}$$

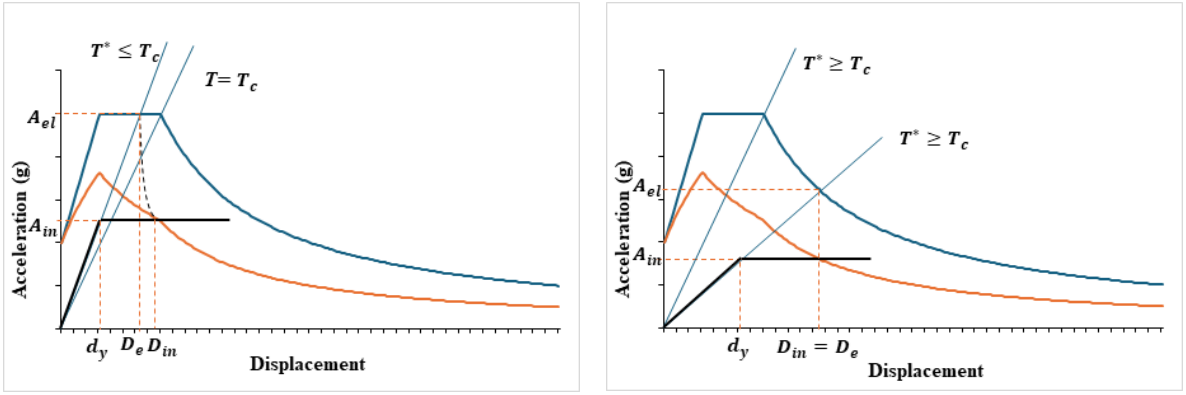

a) b)

Figure 6. a) Seismic demand for equivalent SDOF system with a period in short range b) Seismic demand for equivalent SDOF system with a period in medium/long-period range

Then, the MDOF system's displacement demand is determined using equations (13) and (14).

Pushover analysis is then performed until target displacement is reached, after which resistant capacity and floor drifts are verified.

4.3. Pushover analysis modelling and results

The pushover analysis was conducted in SAP2000 [14]. The structure is regular in plan and elevation and vibrates predominantly in the first mode, therefore, pushover analysis is applicable. A single three-bay moment resisting frame with the shear walls is analysed. P-Δ effects were not included in the analysis as the structure is not sensitive to its effects [9]. Half of the overall structural mass was taken into account.

Non-linear plastic hinges were assigned at the ends of the MRF's beams and columns. The shear walls were modelled with link elements. The behaviour of the link element is determined by the capacity curve obtained from the non-linear analysis of the individual shear wall in Abaqus software, as shown in Fig. 5. c).

The load pattern is defined using equation (6) by determining the diagonal mass matrix and the first mode of the structure, which is determined by conducting the modal analysis. The load is applied using the displacement control method. The structure is loaded until the roof displacement of 0.3 m is reached. The first model used a shear wall with concrete C25/30 and 1 mm thick steel sheets. In the second model, a shear wall with concrete C25/30 and 3 mm thick steel sheets was used, and in the third model, a shear wall with concrete C30/37 and a 3 mm thick steel sheet was used.

During the analysis, in all three models, yielding was not observed in the MRFs, while the shear walls yielded. Therefore, all three systems satisfy the requirements of dual systems.

DOI: https://doi.org/10.5592/CO/3CroCEE.2025.105

The analysis results are represented with so-called capacity curves, showing the relationship between base shear and rooftop displacement. Seismic demand is given for the SDOF system. Therefore, the capacity curve of the MDOF system has to be transformed into the capacity curve of the equivalent SDOF system by using the transformation factor Γ. Using the equal energy principle, the obtained curve is idealised into the bilinear curve. The calculation of yield displacement, elastic periods of the idealised SDOF systems, and target displacements for the equivalent SDOF systems and corresponding MDOF systems are presented in Table 3. Fig. 8. shows the capacity curves of the equivalent SDOF system with corresponding bilinear curves.

Table 3. Calculation of the target displacement [15]

	CCFSSW_03_01_16	CCFSSW_03_03_16	CCFSSW_03_03_16_C30/37
m^*		763.88	
Γ		1.262	
E_m^*	191.37	209.66	232.256
d_m^*	0.23772	0.23772	0.23772
F_y^*	854.6	948.5	1051
$d_y^* = 2(d_m^* - E_m^*/F_y^*)$	0.028	0.033	0.033
$T^* = 2\pi\sqrt{(m^* d_y^*/F_y^*)}$	0.99	1.03	0.98
$S_e(T)$	2.97	2.85	3
$d_{et}^*{}_{SDOF} = S_e(T^*)(T^*/2\pi)$	0.073	0.077	0.073
$d_{et}^*{}_{MDOF} = \Gamma d_{et}^*{}_{SDOF}$	0.092	0.097	0.092

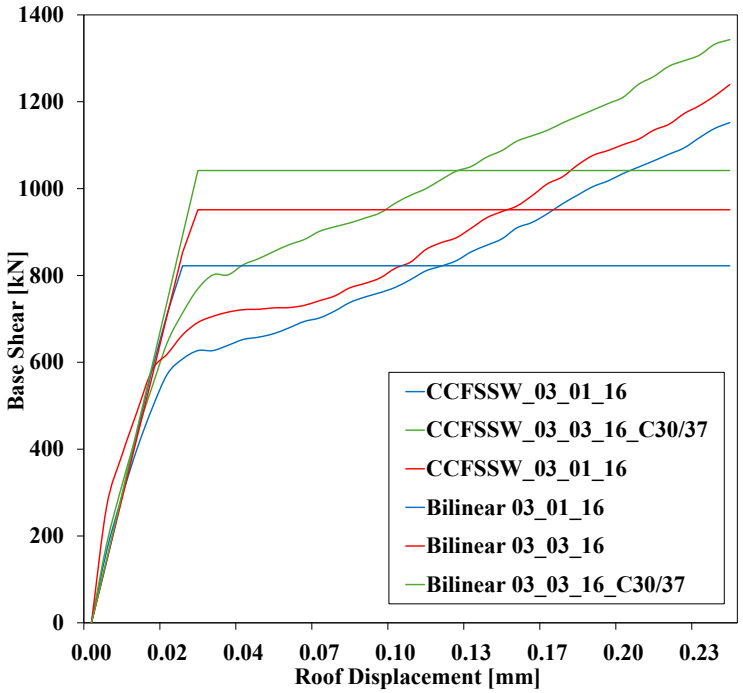

Figure 7. The capacity curves for equivalent SDOF systems and corresponding bilinear idealisations

The overstrength factor can be determined by comparing the base shear at the formation of the plastic mechanism and the base shear at the beginning of the yielding. After obtaining the overstrength factor, the behaviour factor can be calculated as presented in Table 4.

Table 4. Calculated behaviour factors [15]

	CCFSSW_03_01_16	CCFSSW_03_03_16	CCFSSW_03_03_16_C30/37
α_u/α_1	1.35	1.31	1.28
q_0		$4.5 \cdot \alpha_u/\alpha_1$	
$q = q_0 \cdot k_w$, $k_w = 1.00$	6.1	5.9	5.8

DOI: https://doi.org/10.5592/CO/3CroCEE.2025.105

Pushover analysis proved that all three models satisfy the requirements of the dual systems. The shear walls yielded while MRFs remained elastic, thus enabling re-centering. The most notable difference is in the capacity. Comparing the capacity curves of the global models, presented in Fig. 8., with the capacity curves of the individual shear walls, presented in Fig. 5. c), it is evident that the two correlate. The difference in the overstrength ratio and the behaviour factor is not significant. Obtained values of the behaviour factors suggest that the structures can be designed using much smaller forces.

5. Conclusions

Dual structural systems have shown increased attention in recent years because of their re-centring capabilities. The paper analyses dual systems based on finite element analysis that integrate multi-story MRFs with innovative double-skin cold-formed steel concrete composite shear walls. The steel frame consists of three bays, a central braced frame, and two adjacent moment-resisting frames. The shear wall, acting as a bracing system, consists of corrugated cold-formed steel sheets filled with concrete, which are connected with intermediate shear connectors and form a sandwich steel-concrete-steel panel. In this system, the double skin composite shear wall has the function of energy dissipation during an earthquake, while the MRFs remain elastic to provide re-centring forces once the shear walls are removed from each floor. Pushover analysis confirmed the system's dual behaviour. All three shear walls proved to be an effective form of lateral stabilisation. The behaviour factors and overstrength ratios are similar for all three models. The only significant difference is in the capacity of the system, which correlates with the capacity of the individual shear wall. The increase in capacity of the individual shear wall and the global system is achieved primarily by increasing concrete strength, while steel sheet thickness and bolt diameter contribute less. Such structures have the potential of high sustainability after a significant earthquake since replacing the dissipative elements restores the structure to its original position. This paper highlights the benefits of systems with re-centring capabilities, emphasising their potential to reduce repair costs and enhance sustainability. However, further research is needed to optimise these systems and explore different shear wall typologies, which could provide deeper insights into their practical applications.

References

[1] Lukačević I, Maleta T, Dujmovic D. Behaviour of dual eccentrically braced steel frames with short and long seismic links, 2019, p. 1673–80. https://doi.org/10.2749/newyork.2019.1673.

[2] Chesoan A, Stratan A, Dubina D. Design implementation of re-centring dual eccentrically braced frames with removable links. Soil Dynamics and Earthquake Engineering 2018;112:174–84. https://doi.org/10.1016/j.soildyn.2018.05.015.

[3] Dubina D, Dinu F. Experimental evaluation of dual frame structures with thin-walled steel panels. Thin-Walled Structures 2014;78:57–69. https://doi.org/10.1016/j.tws.2014.01.001.

[4] Androić B, Dujmović D, Lukačević I. Projektiranje spregnutih konstrukcija prema Eurocode 4. Zagreb: IA Projektiranje; 2012.

[5] Zhang W, Mahdavian M, Li Y, Yu C. Experiments and Simulations of Cold-Formed Steel Wall Assemblies Using Corrugated Steel Sheathing Subjected to Shear and Gravity Loads. Journal of Structural Engineering 2017;143. https://doi.org/10.1061/(ASCE)ST.1943-541X.0001681.

[6] Zhang W, Mahdavian M, Lan X, Yu C. Cold-Formed Steel Framed Shear Walls with In-Frame Corrugated Steel Sheathing. Journal of Structural Engineering 2021;147. https://doi.org/10.1061/(ASCE)ST.1943-541X.0003182.

[7] Vlaho Žuvelek, Ivan Ćurković, Ivan Lukačević, Andrea Rajić. Numerical Investigation of Double-Skin Cold-Formed Steel Shear Wall Filled with Concrete. In: Ungureanu V, Bragança L, Baniotopoulos C, Abdalla KM, editors. International Conference" Coordinating Engineering for Sustainability and Resilience", Springer Nature Switzerland; 2024, p. 105–15.

[8] ABAQUS User Manual 2014.

DOI: https://doi.org/10.5592/CO/3CroCEE.2025.105

[9] Emanuel Krupa-Jurić. Non-linear analysis of multy-storey steel building with innovative shear wall bracing system. University of Zagreb, Faculty of Civil Engineering, 2024.

[10] Ivan Lukačević, Marko Bartolac, Ivan Ćurković, Andrea Rajić, Vlaho Žuvelek. Laboratory Tests of Lightweight Composite Floor System LWT-FLOOR. Zagreb: n.d.

[11] Lukačević I, Ćurković I, Rajić A, Bartolac M. Lightweight Composite Floor System-Cold-Formed Steel and Concrete-LWT-FLOOR Project. Buildings 2022;12:209. https://doi.org/10.3390/buildings12020209.

[12] Mitrović S, Čaušević M. Non-linear static seismic analysis of structures. Građevinar 2009:521–31.

[13] Fajfar P. Structural analysis in earthquake engineering – a breakthrough of simplified non-linear methods. 12th European Conference on Earthquake Engineering, Elsevier Science Ltd.; 2002.

[14] SAP2000 Integrated Software for Structural Analysis and Design, ” Computers and Structures Inc., Berkeley, California. n.d.

[15] Eurocode 8: Design of structures for earthquake resistance - Part 1: General rules, seismic actions and rules for buildings n.d.